

Study of the mesomorphic phase of PET using DSC and XRD techniques

M. Sahoo^{1(*)}, B. Mallick², G. N. Dash³ and T. N. Tiwari⁴

^{1,3}School of Physics, Sambalpur University, JyotiVihar, Burla 768019, India

²Institute of Physics, Sachivalaya Marg, Bhubaneswar 761005, India

⁴Unique Research Centre, Rourkela-769014, India

Abstract: In this paper, we report the determination of mesomorphic phase (third phase of polymers) using Differential Scanning Calorimetry (DSC) and X-Ray Diffraction (XRD). Various authors have confirmed the existence of mesomorphic phase in polymers using XRD, solvent absorption and FT-Raman scattering techniques. Although, in an earlier work, a broad endothermic peak of polyethylene terephthalate (PET) (below T_g) was observed in the DSC thermogram, no attempt has yet been made to estimate the amount of mesomorphic phase, for lack of proper theory. In this paper, we report the percentage increase in the mesomorphic phase (%M) of both virgin and 2.4 MeV proton-irradiated PET microfibrils measured by DSC, and the results have been compared with XRD technique.

Keywords: PET . Mesomorphic phase . Proton irradiation . DSC . XRD

I. Introduction

Polyethylene terephthalate (PET) is a two-phase material, crystalline and amorphous. In addition to the amorphous (disordered) and crystalline (3-dimensionally-ordered) phases, there is a third phase, referred to as the mesomorphic phase, consisting of a 2-dimensionally-ordered structure [1]. As reported earlier [2], this mesomorphic phase of PET microfibre can be enhanced by proton irradiation. We have chosen this for irradiation because of its wide application in various fields such as textiles [3], surgical polymeric textiles [4], composites [5], nanocomposites [6], conducting polymers [7], electroactive polymers and so on. Polymers can be modified by proton irradiation [8], and the modified polymers possess improved mechanical, electrical, thermal, optical and chemical properties. Again, microfibrils are manufactured to replace traditional materials in applications from super absorbent diapers to artificial organs.

Thermal analysis covers a range of analytical techniques that provide information about materials and thermodynamic properties (exothermic or endothermic) by measuring the changes in their structure and properties in response to change in temperature. The heat of reaction or enthalpy of transition is directly related to the area under the differential scanning calorimetry (DSC) curve. As the mesomorphic phase is a 2-dimensionally-ordered structure, the breaking of this ordered structure shows either endothermic or exothermic reaction, depending on the polymer type. The mesomorphic phase of PET shows an endothermic transition in the DSC thermogram. The appropriate theory related to mesophase structure is described below.

II. Theory

2.1 Thermal technique

Let us consider H_{endo} and H_{exo} as the total heat absorbed during all endothermic and the total heat evolved during all exothermic reactions, respectively. Then the total heat absorbed during this process can be written as

$$H_{endo} = (H_{m, total} + H_{meso, total}) \quad (1)$$

where $H_{m, total} (J) = H_m (J/g) \times w_s$ (heat of melting of crystalline phase), and $H_{meso, total} (J) = H_{meso} (J/g) \times w_s$ (heat of melting of mesomorphic phase), with w_s being the weight of the PET microfibre sample. In the present observation, total heat evolved (H_{exo}) is equal to the total heat evolved during crystallization ($H_{c, total}$) and can be written as

$$H_{c, total} (J) = H_c (J/g) \times w_s \quad (2)$$

Hence, the heat given off for melting the solid polymer $H_{endo} - H_{c, total} = H'_m (J)$. Again, let H_m^* be the heat of melting or fusion, i.e., the amount of heat absorbed by one gram of polymer. According to ATHAS DATA BANK [9], the value of H_m^* for PET is 139.98 J/g. So the crystalline mass (m_c) and its fraction (f_c) can be written as

$$\frac{H'_m (J)}{H_m^* (J/g)} = m_c (g) \quad (3)$$

and $f_c = m_c / m_{total}$

Hence, the percentage crystallinity (%C) can be written as $f_c \times 100$. Again, the total amorphous fraction ($f_a + f_m$) can be written as

$$f_a + f_m = 1 - f_c \quad (4)$$

Moreover, the amount of mesomorphic phase can be written as

$$\frac{H_{meso, total} (J)}{H_m^* (J/g)} = m_m (g), \quad (5)$$

so the fraction f_m can be evaluated as $f_m = m_m / m_{total}$. Hence, the percentage mesomorphic phase, i.e., %M ($= f_m \times 100$) of the sample can be calculated.

2.2 X-ray technique

X-ray scattering takes place coherently from the three different regions of polymer, namely, crystalline, paracrystalline (mesophase) and amorphous [10]. Therefore, the amplitude of X-ray scattered in the direction of scattering vector S by the polymer can be written as

$$A(S) = A_c(S) + A_m(S) + A_a(S) \quad (6)$$

where $A_c(S)$, $A_m(S)$ and $A_a(S)$ are the amplitudes of X-rays scattered by the atoms in crystalline, mesophase and amorphous regions of the polymers respectively. The intensity of X-rays scattered in the direction of S can be written as

$$I(S) = \sum_i \sum_j A_i^j(S) A_i^{j*}(S), \quad (7)$$

where i and j correspond to atoms in a particular type of the above domains of polymers.

According to the model proposed [10], the total intensity scattered in a given direction will be the sum of the total scattering from crystalline domains, mesophase domains and amorphous domains, respectively, and is defined as

$$\begin{aligned} I(S) &= \sum_c \sum_p A_c^p(S) A_c^{p*}(S) + \sum_m \sum_q A_m^q(S) A_m^{q*}(S) + \sum_a \sum_r A_a^r(S) A_a^{r*}(S) \\ &= I_c + I_m + I_a \end{aligned} \quad (8)$$

where the subscripts c , m and a represent the crystalline-phase, the mesophase and the amorphous-phase domains respectively. The second summations, i.e., \sum_p , \sum_q and \sum_r , represent summations over amplitudes scattered from the atoms in a given domain - crystalline, mesomorphic and amorphous, respectively.

Denoting the degree of crystallinity by x_c , mesomorphy (degree of paracrystallinity) by x_m and amorphity by x_a , we have

$$x_c = I_c / I, \quad x_m = I_m / I \quad \text{and} \quad x_a = I_a / I \quad (9)$$

and the total scattered intensity can be written as $I = x_c I + x_m I + x_a I$.

III. Experimental

3.1 Materials

PET microfibre used for our investigation was obtained from a commercial polyester plant. The term microfibre is identified by the term microdenier and refers to synthetic fibres with a denier (weight in gram of 9000 meter of yarn) per filament (dpf) of less than one; however, it is often used for any fibre between 0.5 and 1.5 dpf. The microfibre used for our irradiation study was of draw-twisting-yarn type with a denier value of 0.93dpf.

3.2 Proton irradiation

A proton beam of 2.4MeV energy was obtained from the 3MV tandem-type pelletron accelerator to carry out irradiation in air [11]. The PET microfibre was irradiated for two different fluences 1.5×10^{11} p/cm² and 1.5×10^{12} p/cm² at normal atmospheric pressure and temperature (ranging between 18-22 °C). The beam was initially collimated by a graphite collimator to a beam size of 3 mm diameter and was extracted into air using a Kapton™ foil of 8 micron at the exit point of the vacuum (1×10^{-6} mbar) chamber. The external beam current measurement was performed using a rotating vane chopper designed at the Institute of Physics, Bhubaneswar. Beam size of the external proton beam can be increased up to 10-15mm diameter circular patch by proper adjustment. In the present study, the beam was allowed to travel 3 cm in air inside the irradiation cell (an aluminum cylinder of 15mm diameter and 30mm length) rotating with 1Hz frequency for homogeneous irradiation, during which the energy gets reduced to about 2.4MeV before interaction with the microfibre. Calculation of projectile range in air and the materials was done using the “TRIM” program.

3.3 Characterization

A Netzsch STA 409C simultaneous thermal analyzer, which combines simultaneous thermogravimetry and Differential Scanning Calorimetry [12] with a temperature range of 0 to 1600 °C, was used to measure the mass profile and reaction temperatures of the materials. The experiments were performed in a nitrogen atmosphere with a flow rate of 80ml/min, operated in the range of 25 °C to 325 °C at a heating rate of 5 K/min. Microfibre sample of 15mg was taken in an Alumina crucible for the testing. NETZSCH-TA windows software version 3.5 was used for thermal analysis of virgin (I) and irradiated (II and III) samples.

The X-ray diffraction patterns were obtained for both non-irradiated (I) and irradiated (II) PET microfibre using a PANalytical X-ray Diffractometer (X'Pert-MPD) employing Bragg–Brentano parafocusing optics. The X-ray diffraction patterns were recorded with a step size of 0.01° on a 3°-55° range with a scanning rate of 0.5°/min. Line focus CuK_α-radiation from an X-ray tube (operated at 40 kV and 30 mA) was collimated through Soller slit (SS) of 0.04 rad., fixed divergence slit of 0.5° and mask (10 mm) before getting it diffracted from the sample. Then, the diffracted beam from the sample was well collimated by passing it through a programmable anti-scattering slit of 1°(to reduce air scattering), programmable receiving slit of 0.15mm and Soller slit of 0.04 rad., before getting it reflected by the curved graphite crystal (002) monochromator of radius 225mm for high resolution diffraction study. A Xe-gas-filled proportional counter was mounted on the arm of the goniometer circle of radius 200mm to receive the diffracted X-ray signal. Experimental control and data acquisition were fully automated through a computer.

IV. Results and discussion

4.1 Thermal analysis

The glass transition temperature (T_g) and melting temperature (T_m) of virgin sample are observed to be 92.9 °C and 254.6 °C, respectively. The broad endothermic peak was observed below T_g in the DSC thermogram of the virgin sample as shown in fig.1 (a). The T_g was calculated by taking the arithmetic mean of the extrapolated ONSET and ENDSET of the glass transition phase in the midpoint of the DSC curve using NETZSCH-TA software. No variation has been observed in T_g value in this irradiation range, whereas the T_m value slightly increases with proton irradiation. Though the cold crystallization peak was not observed in virgin sample (I), it was clearly shown at 190 °C in the DSC thermogram of irradiated sample (II) as shown in fig. 1(b). Again, the change in specific heat ΔC_p value at glass transition (fig. 1(c)) was calculated using the above software. The DSC peak area is proportional to the change in enthalpy ΔH , i.e., the total heat consumed (endothermic) or released (exothermic) by the sample, and can be written [13] as $\Delta H = \frac{A}{m K_{calib}}$, where A is

the peak area, K_{calib} is the calibration factor and m is the mass of the sample.

The enthalpy of melting ΔH_m for the virgin sample was found to be 33.61 J/g. The ΔH_m value increased to 39.02 J/g and 41.07J/g when the microfibre was irradiated with a fluences of 1.5×10^{11} p/cm² and 1.5×10^{12} p/cm², respectively, which may be attributed to the degradation. The increase in ΔH_m indicates the

proton-induced crosslinking after irradiation in air, which gives the material increased thermal stability, due to which strong-fibre materials are likely to be formed.

The broadening of the above-said endothermic peak (below T_g) increases (fig. 1(d)) with proton fluences. Although the above broad endothermic peak, was observed by earlier workers [14] in their study of PET, no attempt to estimate the amount of mesomorphic phase that exists in the material was done, for the lack of proper theory in earlier days. The PET is semi crystalline (partially crystalline) in nature. The crystalline percentage of PET materials can be written [12] as $\%C = \frac{\Delta H_m - \Delta H_c}{\Delta H_m^0}$, where ΔH_m is the measured enthalpy of melting of the material., ΔH_c is the enthalpy of the cold crystallization observed during the DSC run and ΔH_m^0 is the standard enthalpy of the melting of wholly (100% pure) crystalline materials, ($\Delta H_m^0 = 139.98$ J/g, for PET [9]).

Again, the crystalline (%C), amorphous (%A) and mesomorphic (%M) phase percentages has been calculated for all the samples and are presented in Table 1.

4.2 X-ray analysis

Changes in the peak position and intensity were obtained in the X-ray diffraction pattern, as shown in fig. 2, of the irradiated PET fibre as compared to the virgin. Again, a low-intensity, broad X-ray diffraction peak was observed at low angle ($2\theta = 6^\circ$) in the case of the irradiated microfiber, keeping the fibre axis parallel to the incident X-ray beam, and was not observable when the fibre was kept perpendicular to the incident X-ray beam. This fact indicates the presence of mesomorphic phases. In the case of proton irradiation, it is also observed that the $d(A^\circ)$ values increase with fluences like neutron [15] because of the development of microstrain due to radiation heating. The crystalline (%C), amorphous (%A) and mesomorphic (%M) phase percent of PET microfibre was calculated from the peak area of all samples.

Crystallinity of virgin and proton-irradiated samples has been calculated using $\%C = \frac{\Delta H_m - \Delta H_c}{\Delta H_m^0}$,

and their values are given in the Table 1. In this case, the crystallinity calculated by XRD was found to be less as compared to DSC. This is because of the subtraction of mesophase contribution to the crystallinity calculated by XRD technique. The percentage of mesomorphic phase measured by above DSC technique was found to be less as compared to XRD. This may be due to contribution of some other factors such as macromolecular orientation, chain-folding mechanism etc., which cannot be measured by DSC. But the trend report of the results has been given in Koptelov and Shlenski [16], where the crystallinity of gamma-irradiated polyterafluoroethylene sample, measured by XRD technique, is quite higher than that measured by DSC technique.

As discussed in the earlier theory of DSC, this may be due to the formation of radiation-induced microstrain, or chain-folding factors, which affect crystallinity measured by X-ray diffraction, but not the measurement by DSC technique. However, the phase (C+M) value measured by XRD and DSC have matched well with trend of Koptelov and Shlenski [16].

V. Conclusions

It is confirmed from the DSC results that the area of the endothermic peak (below T_g) of PET microfibre increases with proton fluences. This indicates enhancement in the percentage of mesomorphic phase due to 2.4 MeV proton irradiation for both the fluences, i.e., 1.5×10^{11} p/cm² and 1.5×10^{12} p/cm². The percentage of mesomorphic phase (%M) has been calculated using the above given formula based on DSC principle. The parameter has also been calculated by XRD along with the percentage of crystallinity (%C). The latter is found to increase linearly with proton fluences, similar to the DSC results. The increase of T_m is indicative of the improvement in the thermal stability of microfibre due to proton irradiation. The present study on mesomorphic phase will help to understand the optoelectronic behavior of polymers for sensor applications.

Acknowledgements

Authors would like to thank Technical staff of the Department of Metallurgical and Materials Engineering, National Institute of Technology, Rourkela, and the Scientific & Technical staff of the Ion Beam Laboratory, Institute of Physics, Bhubaneswar, for their help during the experimental work.

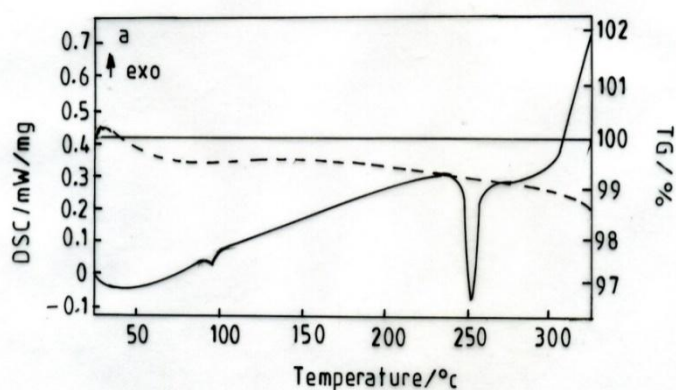
References

- [1]. A. Brookes, J.M.Dyke, P.J. Hendra and S. Meehan , The FT-Raman spectroscopic study of polymers at temperatures in excess of 200° C, Spectrochim. Acta. A. 53(1997)2313.
- [2]. B. Mallick, T. Patel and R.C. Behera, Mesomorphic phase sensitivity of polymer microfiber to proton irradiation, WW-EAP Newsletter (NASA). 6(2004)18.
- [3]. T. Patel and S. Bal , Comparative study of structural parameters of normal and alkali-treated polyester fiber by SAXS, SEM and Instron. Polym. J.33(2001)121.
- [4]. L.M. Ferreira, M.H. Casimiro, C. Oliveira, M.E. Cabeco Silva, M.J. Marques Abreu and A.Coelho, Thermal analysis evaluation of mechanical properties changes promoted by gamma radiation in surgical polymeric textiles, Nucl. Instr. and Meth. B. 191(2002)675.
- [5]. S. Fu, P. Wu and Z. Han, Tensile strength and rupture energy of hybrid poly(methylvinylsiloxane) composites reinforced with short PET fibers and wollastonite whiskers, Compos. Sci. Technol. 62 (2002) 3.
- [6]. J. H. Chang, S. J. Kim, Y. L. Joo and S. S. Im, Poly(ethylene terephthalate) Nanocomposites by in-situ interlayer polymerization: the thermo-mechanical properties and morphology of the hybrid fibers, Polymer. 45 (2004) 919.
- [7]. R. Mishra, S.P. Tripathy, D. Sinha, K.K. Dwivedi, S. Ghosh, D.T. Khathing, M. Muller, D. Fink and W. H. Chung, Optical and electrical properties of some electron and proton irradiated polymers, Nucl. Instr. and Meth. B. 168 (2000) 59.
- [8]. M.E. Martinez-Pardo, J. Cardoso, H. Vazquez and M. Aguilar, Characterization of MeV proton irradiated PS and LDPF thin films, Nucl. Instr. and Meth. B. 140 (1998) 325.
- [9]. ATHAS DATA BANK, Internet databank (Advanced Thermal Analysis System (ATHAS), Last revision February 5, 2000 by Marek Pyda, <http://web.utk.edu/~Athas/databank/Intr.Html>) (2002).
- [10]. G.B. Mitra and P.S. Mukherjee, X-ray diffraction study of fibrous polymers. I. Degree of paracrystallinity- a new parameter for characterizing fibrous polymers. Polymer. 21 (1980) 1403.
- [11]. V. Vijayan, R.K. Choudhury, B. Mallick, S. Sahu, S.K. Choudhury, H.P. Lenka, T.R. Rautray and P. K. Nayak, External particle-induced X-ray emission, Curr. Sci.85 (2003) 772.
- [12]. G.W.H. Hohne, W.F. Hemminger and H.J. Flammersheim, Differential Scanning Calorimetry, Springer, London, 2003.
- [13]. NETZSCH-Gerätebau GmbH, NETZSCH-TA windows software, version 3.5, 1999.
- [14]. J. Runt, I.R. Harrison, in: R. A. Fava (Ed.). Thermal analysis of polymer (Methods of Experimental Physics: Polymers), Vol.16, Part B, Academic Press, New York, 1980.
- [15]. B. Mallick, R.C. Behera and T. Patel, Analysis of microstress in neutron irradiated polyester fiber by X-ray diffraction technique. Bull. Mater. Sci. 28 (2005) 593.
- [16]. A.A. Koptelov and O.F. Shlenskii, The crystallinity of γ -Irradiated poly(tetrafluoroethylene). High Energy. Chem 36 .(2004) 217.

Table (1) DSC and XRD data of PET microfibre

Sample	Fluence p/cm ²	DSC					XRD			Phase% [†]	
		T _g (°C)	T _m (°C)	ΔC_p (J/g. °K)	ΔH_m (J/g)	ΔH_c (J/g)	d(A°)	2 θ (deg.)	h k l	DSC	XRD
I	0	92.9 ±0.2	254.6 ±0.2	0.14 ±0.02	33.61	-	5.0776	17.45	010	37.15(c)	31.69(c)
							3.9170	22.68	110	49.73(a)	45.54(a)
							3.4627	25.71	100	13.13(m)	22.77(m)
II	1.5×10 ¹¹	92.5 ±0.2	255.8 ±0.2	0.17 ±0.02	39.02	4.456	5.0978	17.38	010	40.01(c)	32.14(c)
							3.9471	22.51	110	43.18(a)	39.76(a)
							3.4941	25.47	100	16.81(m)	28.00(m)
III	1.5×10 ¹²	92.6 ±0.2	255.7 ±0.2	0.13 ±0.02	41.07	5.086	5.1079	17.35	010	42.34(c)	34.14(c)
							4.0014	22.20	110	37.06(a)	34.25(a)
							3.5037	25.40	100	20.60(m)	31.61(m)

[†]The bracketed letters, viz., (c), (a) and (m) are used for crystalline, amorphous and mesomorphic phases, respectively.



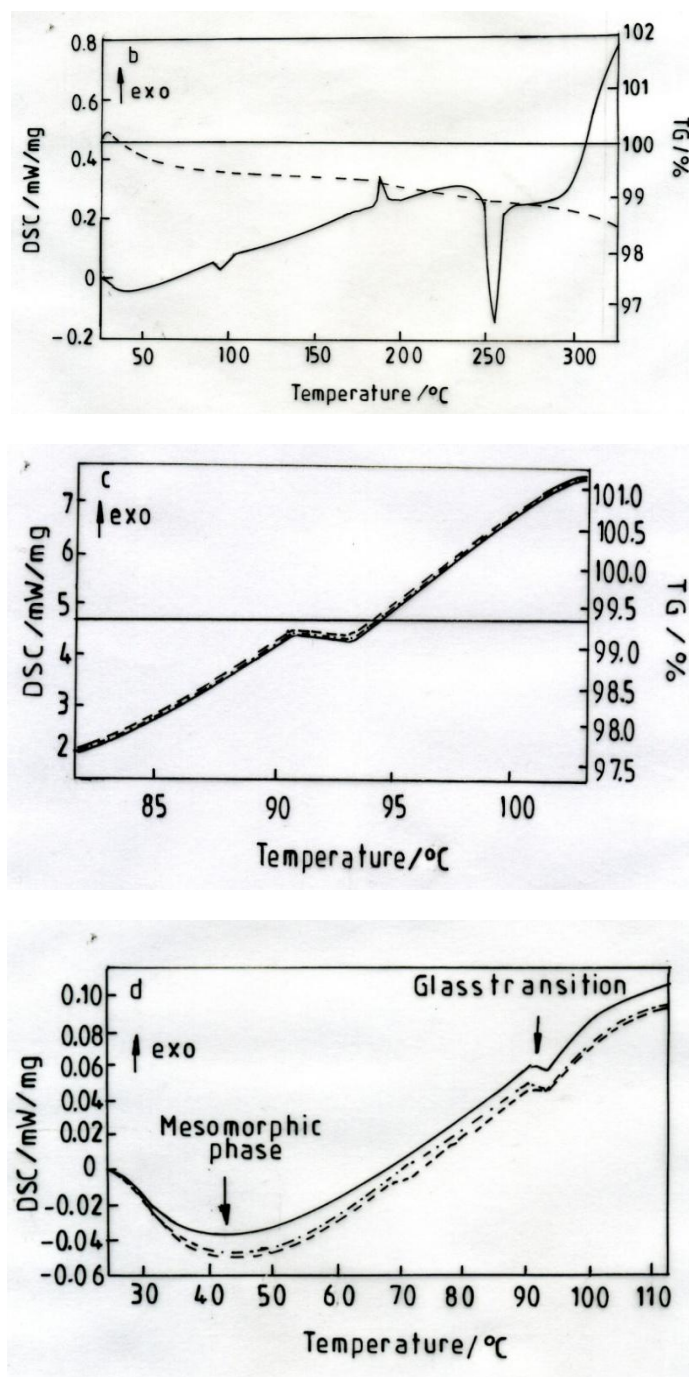


Figure 1 DSC (—) and TG (---) curve of (a) virgin (I) and (b) irradiated (II) PET microfibre sample. (c) The glass transition plot of sample III and (d) endothermic transition due to mesomorphic phase of sample I (—), II (····) and III (---).

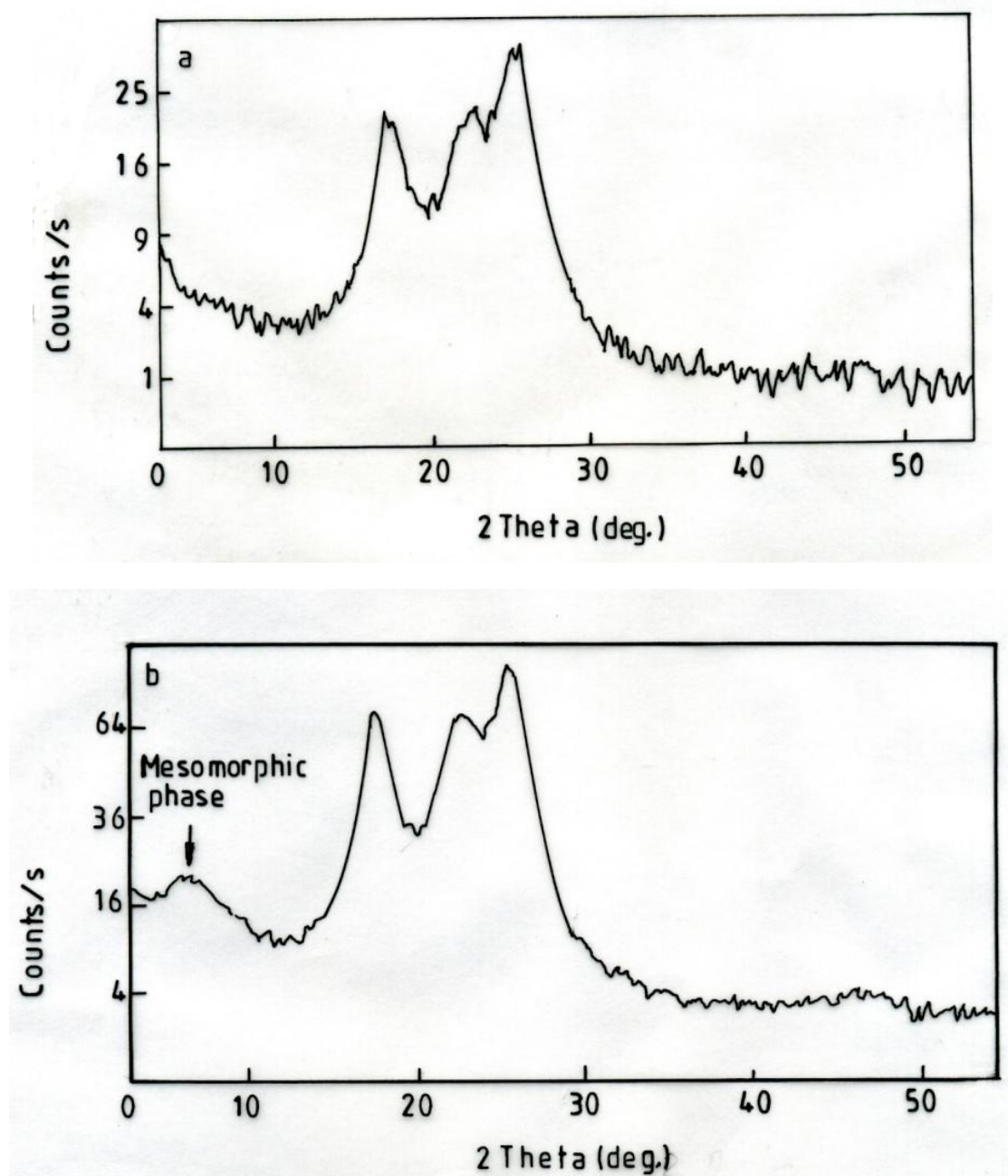


Figure 2 (a) X-ray diffraction pattern of sample I and (b) X-ray diffraction pattern of sample III

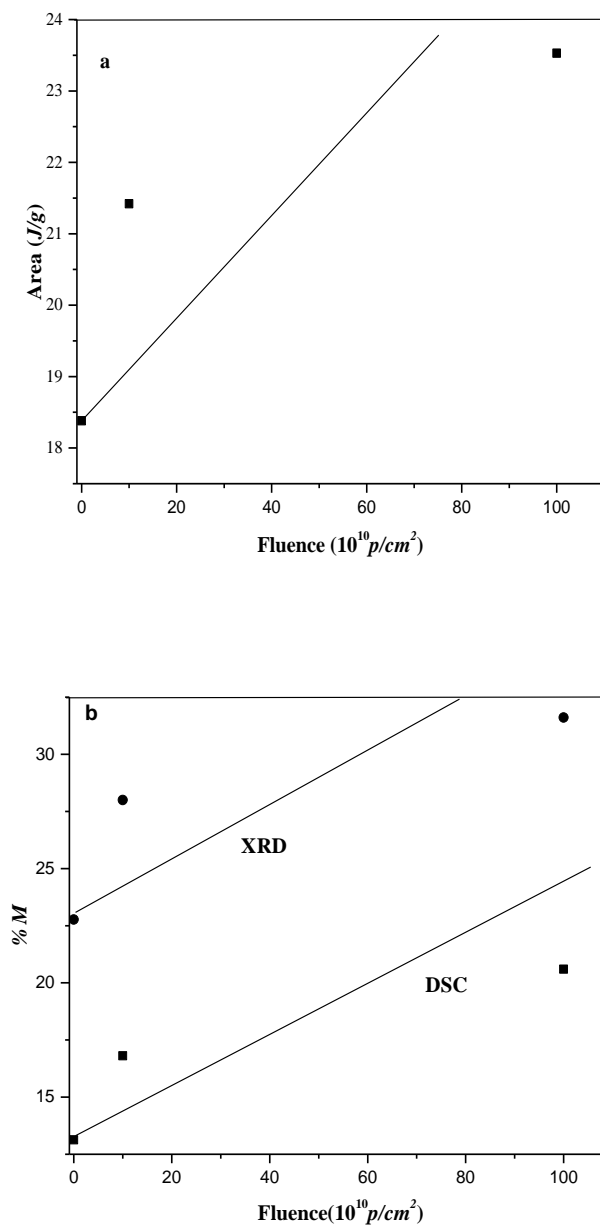


Figure 3 (a) Fluence vs. endothermic peak area (change in enthalpy) and (b) fluence vs. percent mesomorphic phase (%M).